

# On the Relation between the African ITCZ and the Development of a Medicane “Scott” storm over east Mediterranean: case study

Abdulahleem Hussin Labban

Department of Meteorology, King Abdulaziz University, P.O. Box 80234, Jeddah 21589, Saudi Arabia  
alabban@kau.edu.sa, <https://orcid.org/0000-0003-0072-6306>

**Abstract.** the present study investigates the role played by the African Intertropical Convergence Zone (AITCZ) in the development of Medicane Scott Landfall over Egypt during the period from 21 to 27 October 2019. The NCEP/NCAR reanalysis of daily precipitation, geopotential height (at 500 hPa), decadal, and daily data of the AITCZ for October 2019 have been used. Time series analysis, anomaly, and correlation coefficient methods were used to analyze these data sets. The results reveal that there is a notable northward extension of the AITCZ, mainly over eastern Africa through the period of Medicane Scott. There is a strong significant positive correlation (0.925) between the daily precipitation over Egypt and the latitudinal position of the eastern part of AITCZ during the period of Medicane Scott. The AITCZ controls the persistence of the Rossby wave over Europe and the Eastern Mediterranean regions causing an omega-shaped block over the southern part of Europe. However, the eastern flank of this block is the Medicane Scott that landfall over Egypt which is associated with severe abnormal rainy weather over Egypt.

**Key words:** Medicane Scott, Precipitation Rate, AITCZ, Omega Shaped Block, Egypt, Mediterranean

## INTRODUCTION

Medicane is a Mediterranean tropical-like cyclone observed over the Mediterranean Sea, where the word Medicane is a combination of two words "Mediterranean" and "Hurricane". In real, tropical-like cyclones (TLC) in the Mediterranean are rarely meteorological phenomena recorded only every few years. On a few times, the storms reached to the force of a Category one hurricane (Cavicchia et al. 2014; Miglietta et al. 2015; Romera et al. 2017; Gaertner et al. 2018; Ricchi et al. 2019). Medicanes are uncommon because of the dry nature of the Mediterranean region, the genesis of tropical, subtropical cyclones, and tropical-like cyclones. Historically, the maximum occurrence of tropical-like cyclones is between September and January, while the minimum occurrence is in the summer months (Cavicchia et al. 2014). Numerical simulations show that the latent heat liberation associated with the convection process and air-sea interaction process is fundamental for the intensification of Medicanes, while the existence of baroclinic instability is important in the early stages of their lifetime during which these cyclones occur under deep upper-tropospheric troughs (Emanuel 2005; Moscatello et al. 2008). Scott touched winds of 75 km/h and pointed with a minimum pressure of 1005 millibar. In addition, a couple of recent papers have elevated some doubts concerning the application of this mechanism to two TLCs (Mazza et al. 2017; Fita and Flaounas 2018), supporting the idea that the warm-air seclusion in the extratropical cyclone's inner core by

surrounding colder air may explain the existence of a deeply warm, core structure.

The intertropical convergence zone (ITCZ), an important component of the general atmospheric cycle in the subtropical and tropical areas, has a band of maximum precipitation and cloudiness around the equator, and it is considered an effective system. Therefore, the position and movement of this system can not only recognize the place of the maximum precipitation lengthwise of the latitude in the tropics, but also spatially and temporally control the occurrence and strictness. The ITCZ plays an important role in determining the flow and patterns of hurricanes and extreme climatic events (Chan and Evans 2002; Hafez 2012a; Hafez and Almazroui 2016; Hafez 2016; Jafari and Lashkari 2020). Henceforward, the position, construction, and resettlement of the ITCZ are important in controlling and inspecting the global climate along with the strength and the atmosphere-sea linking at a local scale (Waliser and Gautier 1993). Moreover, large-scale atmospheric phenomena like the blocking systems have a great role in the existence of extreme climatic events such as hurricanes and extratropical cyclones. The blocking systems may be coursing of extreme rainfall, heat waves, and presenting of low-pressure systems over the globe (Diao et al. 2006; Hafez 2008, 2012b; Barriopedro et al. 2011; Hafez and Labban 2018; Hafez et al. 2020; Woollings et al. 2018).

*The present work aims to investigate the relationship between the African Intertropical Convergence Zone (AITCZ) and the development of Medicane Scott landfall over east Mediterranean in late October 2019.*

## DATA AND METHODOLOGY

Six-hourly of zonal (u) and meridional (v) wind components (m/sec), temperature ( $T^{\circ}\text{C}$ ), specific humidity (q g/kg) and the geopotential height (Z gpm) with horizontal resolution of  $2.5^{\circ} \times 2.5^{\circ}$  over the area bounded by  $20^{\circ}\text{W} - 80^{\circ}\text{E}$  and  $0^{\circ} - 80^{\circ}\text{N}$  from the European Centre for Medium-range Weather Forecasts Reanalysis Interim dataset ERA5 dataset (Hersbach et al., 2020) during the period from 20 to 31 October 2019. These parameters are obtained at 1000, 850, 700, 500, 400, 300, 250, 200, 150 and 100 hPa pressure levels. Daily precipitation data of  $0.25^{\circ} \times 0.25^{\circ}$  horizontal resolution were obtained from Tropical Rainfall Measuring Mission (TRMM-3B42) (Huffman et al. 2010). The African ITCZ ( $15^{\circ}\text{W} - 35^{\circ}\text{E}$ ) mean position data for the period 1979-2001 is used. However, the movement of the AITCZ is monitored by plotting the daily location of the surface  $15^{\circ}\text{C}$  dew point temperature at 1200 UTC for every 5 degrees of longitude (Ilesanmi 1971). For Africa, the mean position for every 10 days is calculated for the region from  $15^{\circ}\text{W}$  to  $35^{\circ}\text{E}$ . The African ITCZ records were obtained from the Climate Prediction Centre ([http://www.cpc.ncep.noaa.gov/products/monitoring\\_data/](http://www.cpc.ncep.noaa.gov/products/monitoring_data/)). Moreover, visible (VIS) satellite images obtained from the European Organization for the Exploitation of Meteorological Satellites (EUMETSAT) were used to identify the daily AITCZ position by using cloud clusters through the period 21st-27th October 2019. In the present work, these datasets are analysed using anomalies and correlation coefficient techniques. The linear correlation method according to Kendall is used. However, a statistical significance was determined by using the Kendall-tau test. According to that test, a trend is deemed to be “statistically significant” if it has at least 90% significance (Bonett and Wright 2000).

To detect the role of the blocking system in the development, of Medicane Scott landfall over Egypt in October 2019, a suitable definition of blocking episode is needed. However, there are several definitions of blocking systems. For the present study, both synoptic and numeric blocking formation criteria are considered. The blocking criteria according to (Rex 1951; Dole and Gordon 1983; Hafez et al. 2018) are used. The synoptic charts of geopotential height conditions at 500 hPa side by side are used to define the anomaly conditions. These criteria have conditions such as the westerly air current aloft must split into two distinct branches. Moreover, to that, for numeric, quantitatively, the anomaly in geopotential height at 500 hPa must be more than +100 m for a high-pressure flag for several longitudes. The anomaly is less than or equal to -100 m for a low-pressure flag for several longitudes. These conditions must persist for five days continually or more. However, this numeric method has precise quantitatively suitable values for blocking detection.

## MOISTURE FLUX CALCULATION

According to Chakraborty et al., 2006 and Abdeldym et al., 2019, the precipitable water content in an air column is calculated as

$$\text{PWC} = \frac{1}{g} \int_{P_u}^{P_L} q \, dp$$

Similarly, zonal and meridional water vapour flux transports are calculated as

$$Q_u = \frac{1}{g} \int_{P_u}^{P_L} qu \, dp$$

And

$$Q_v = \frac{1}{g} \int_{P_u}^{P_L} qv \, dp$$

Where total water vapour transport is  $Q = Q_u i + Q_v j$ .

The total water vapour flux decompose into rotational and divergent components (Rosen et al. 1979; chen, 1985) in terms of the stream function ( $\psi$ ) and velocity potential ( $\chi$ ), we can write

$$Q = kx\nabla\psi + \nabla\chi \quad (4)$$

The  $\psi$  and  $\chi$  fields are obtained from

$$\nabla^2\psi = k \cdot \nabla x Q \text{ and } \nabla^2\chi = \nabla \cdot Q \quad (5)$$

The Equation (9) can be solved easily for  $\psi$  and  $\chi$  using the relaxation method (Krishnamurti and Bounoua, 1997). Finally, rotational and divergent moisture vectors can be derived as

$$Q_u^R = -\frac{\partial\psi}{\partial y}, Q_v^R = \frac{\partial\psi}{\partial x} \text{ and } Q_u^D = \frac{\partial\chi}{\partial x}, Q_v^D = \frac{\partial\chi}{\partial y} \quad (6)$$

Where g acceleration due to gravity; q refers to the specific humidity;  $P_L$  pressure at the bottom of the air column; and  $P_u$  pressure at the top of the air column.

The perceptible water content in an air column within any two pressure layers was calculated using equation 1. To determine the moisture source (divergence) and moisture-sink (convergence) regions of water vapour, we calculate both the divergent and rotational components of moisture transport. To find the components of moisture vectors, first we calculated the total water vapour transport (Q) within any two pressure layers using equations 2 and 3, and then we used equation 5 for stream function ( $\psi$ ) and velocity potential ( $\chi$ ). Finally, we used equation 6 because the stream function and velocity potential are already known.

## SYNOPTIC DISCUSSION

During the period 21–28 October 2019 most of the eastern region of Mediterranean, especially the south and east parts, exposed to heavy rainstorms and reached to about 100 mm during 23–26 October. Figures 1 and 2 show the geopotential height (gpm) in meters with the temperature in  $^{\circ}\text{C}$  on 1000 and

500 hPa levels, while Figure 4 illustrate the horizontal distribution of the geopotential height (gpm) and temperature advection on 850 hPa. Figure 1a shows that, at 12:00 UTC 21 October 2019, the subtropical high pressure extended to cover most area of northeast Africa and east Mediterranean and covered the northern part of Saudi Arabia. Contrarily, the Sudan monsoon low and its associated Red Sea trough (RST) extended northward to cover the southeastern part of Egypt and the Red Sea region. Additionally, there was an obvious thermal gradient (red dashed line) associated with the RST and extended zonally to cover the northern part of Sudan and the southern part of Saudi Arabia (Figure 1a). Simultaneously, the upper air (500 hPa) trough appeared over Turkey as an extension of the traveling depression (Figure 2a). During 21 October, the Sudan monsoon low deepened with slowly northward propagation of RST to cover most Egypt, while the subtropical high-pressure weakened and moved eastward (Figure 1b), this situation sometimes called Medcane Scott (Blakkovic 2019). Figure 3b illustrates that there was an area of cold advection over East Asia, while the warm advection appeared over the Arabian Peninsula and Iran. Furthermore, the 500 hPa cut-off low started to deepen and moved south eastward to cover east

Mediterranean and the northeastern parts of Egypt (Figure 2b). The intense development of surface (1000 hPa) and upper air pressure systems occurred in the beginning of 21 October 2019 and continued until 27 October 2019. At 00:00 UTC 23 October 2019, the surface RST extended northward and covered the northern region of the study domain (Egypt, East Mediterranean, and Saudi Arabia). The Sudan low was centered over south Red Sea with a geopotential height of 60 gpm at its center (Figure 1c). Moreover, the 500 hPa cut-off low deepened more and moved slowly south westward to cover the north of Egypt and East Mediterranean, with a geopotential height of 55800 gpm at its center (Figure 2c). On 850 hPa (Figure 3c), it is clear that the areas of cold advection moved westward with the movement of our cyclone, while a significant warm advection appeared over the Arabian Peninsula, Red Sea, Mediterranean, northwest region of our domain. This pattern of temperature advection continued also at 24 October (Figure 3d), During the period 12:00 UTC 23 October 2019 to 12:00 26 October 2019 (the rainy period), a strong interaction between the extended surface RST from the tropical region (Figure 1c,d,e,f) and upper air

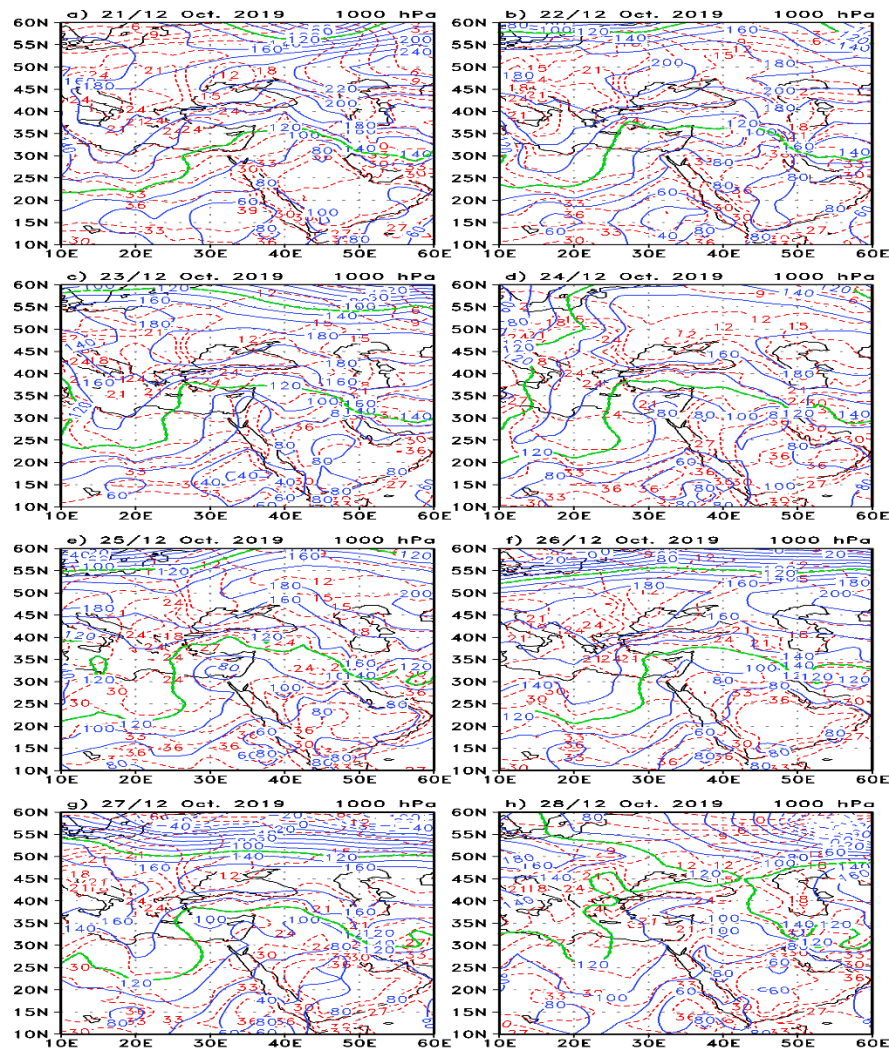


**Figure 1.** 1000 hPa geopotential height with 20 m contour intervals (blue solid lines) and temperature (red dashed lines) every 3 °C (a–h) for the period 21–28 October 2019.

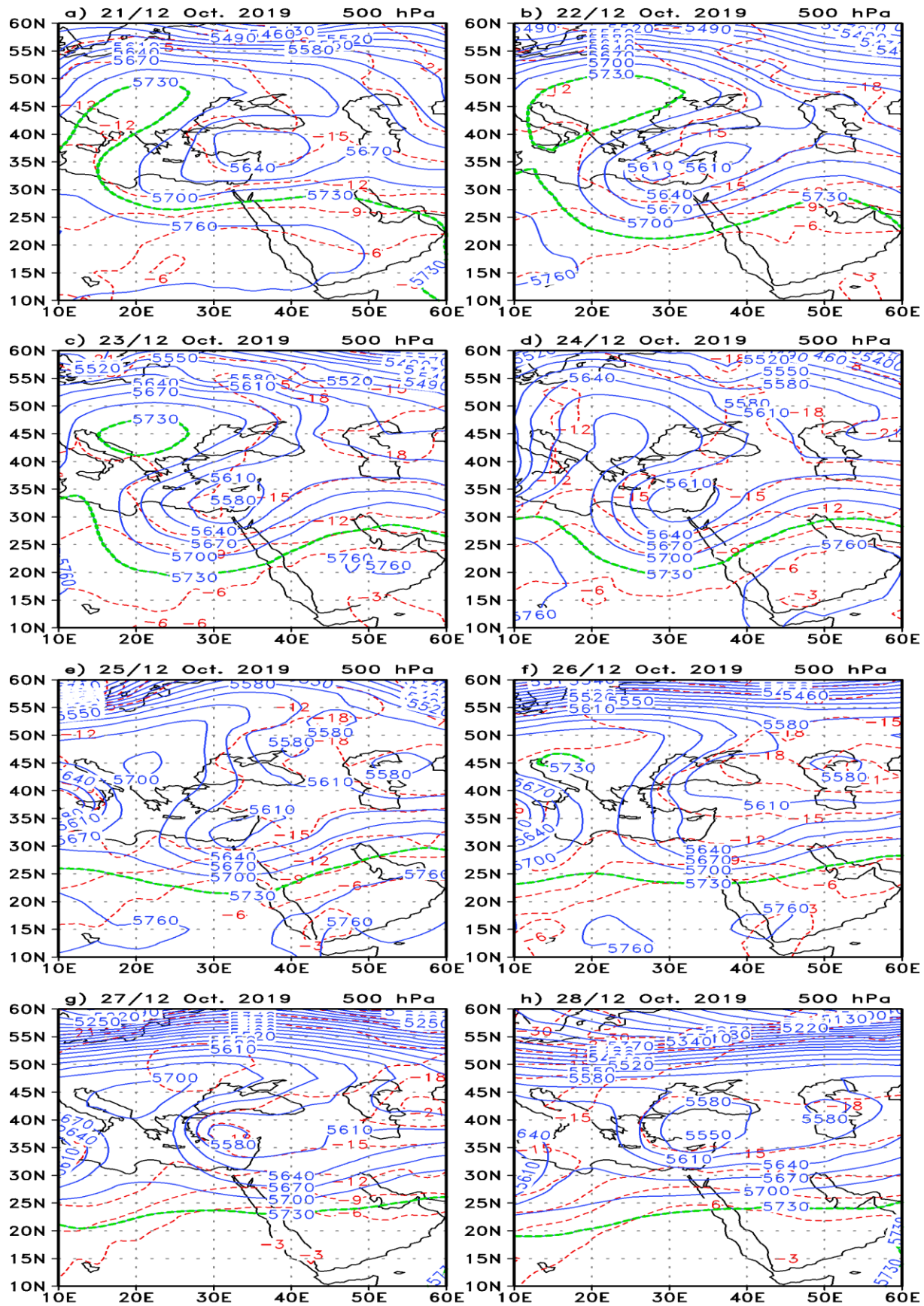


**Figure 2.** 500 hPa geopotential height with 30 m contour intervals (blue and green solid lines) and temperature (red dashed lines) every 3 °C (a-h) for the period 21–28 October 2019.

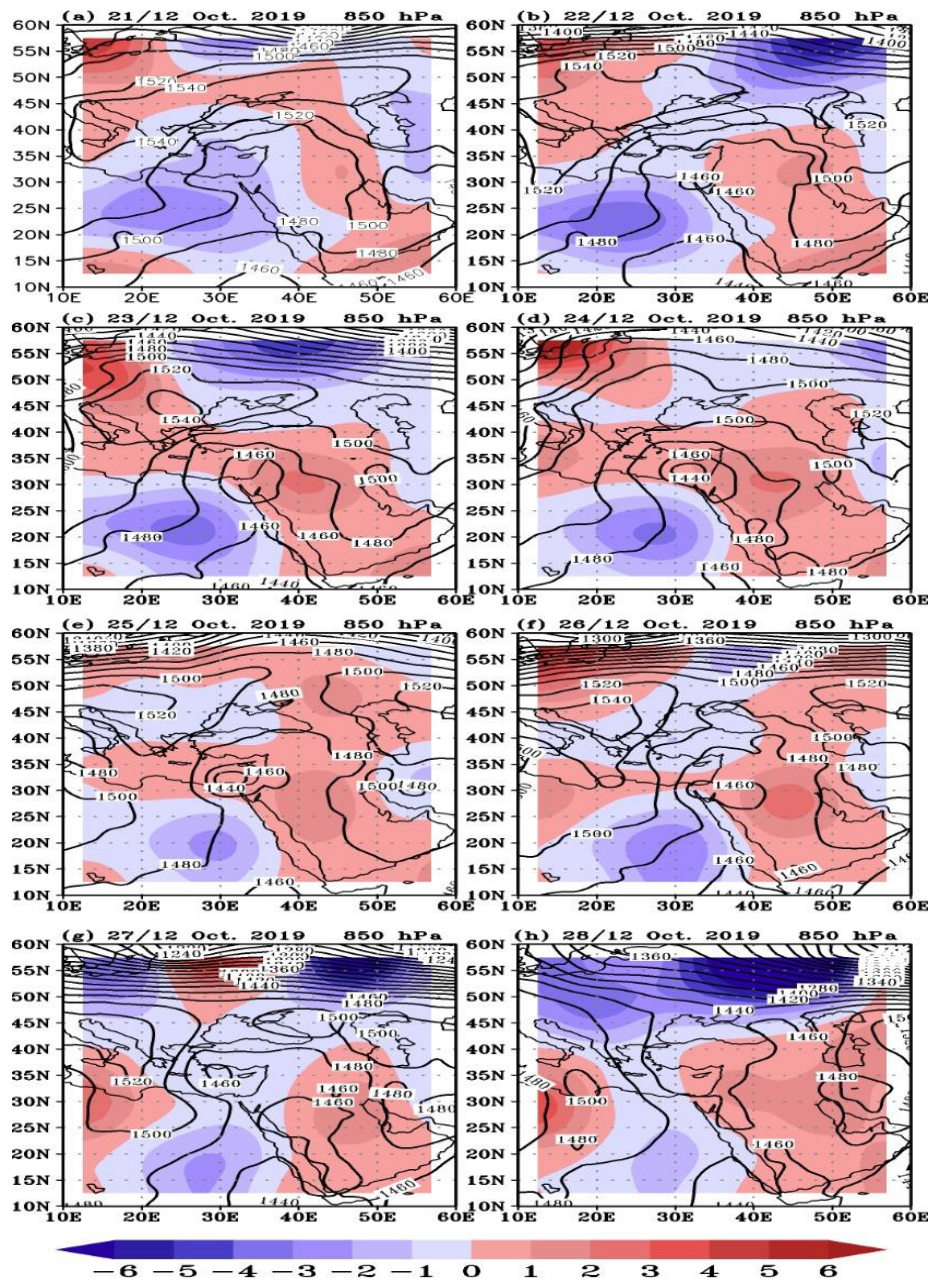


**Figure 3.** 850 hPa geopotential height with 30 m contour intervals (black solid lines) and horizontal advection of temperature (red and blue shaded areas) (a–h) for the period 21–28 October 2019.

trough from mid-latitude region (Figure 2c,d,e,f) occurred and became more intense. These two depressions (RST and upper air trough) amalgamated to build up a single system. The most significant function of the extended RST was the northward transporting of tropical warm and moist air, as well as the upper air trough provides a polar strong southward cold advection (Figure 3c-f). The interaction between these tropical warm and polar cold air masses contributed to intensify the atmospheric instability over the East Mediterranean and Egypt. After 12:00 UTC 26 October 2019, the RST moved southwestward (Figure 1g,h) and the upper air trough moved northeastward (Figure 2g,h), and their interaction vanished and the atmospheric stability and the high-pressure system dominated the region.

## 4. RESULTS AND DISCUSSION

### 4.1 RAINFALL DISTRIBUTION DURING THE PERIOD OF STUDY

During the period from 21 to 28 October 2019, EM and north east Africa (Egypt) suffered from a rare and strong storm, usually, this storm is called Medicane Scott (Blakkovic 2019). However, an area of a low-pressure system appeared and developed over the EM late October 2019. Figure 4 illustrate the spatial distribution of the daily rainfall pattern from the TRMM dataset for the period 21–28 October 2019. The precipitation amounts measure as much as 10 times the October

monthly average over Egypt. This extreme amount of rainfall creates a risk of flooding over several governorates of Egypt. Northeastern portions of Greater Cairo were among the vilest exaggerated besides, Nasr City and regions nearby Cairo's international airport. On 25 October, the Medicane Scott landfall occurred over the coastline west of Port Said, Egypt with maximum sustained winds of 72 km/h and gusts to 80 km/h. Rainfall bands reached south of Cairo (Blakkovic 2019; Mudzwiti 2019; Tonks et al. 2019). Moreover, Cairo international airport's meteorological station recorded a rainfall amount of 4.3 mm on 24 October. Port Said meteorological station recorded 7.3 mm rainfall on 26 October.

26 October. The satellite images onboard NASA's Aqua satellite acquired a true-color image of this storm spinning in the EM and Egypt during the period from 21 to 27 October 2019. Medicane Scott reached its mature stage on Friday 25 October. As shown in Figure 5, the Moderate Resolution Imaging Spectroradiometer (MODIS) on panel NASA's Aqua satellite acquired a true-color image of the storm-turning region of the Eastern Mediterranean Sea on October 25th,

Figure 5 shows the Satellite images of the daily position of Medicane Scott over Eastern Mediterranean for the period 21-

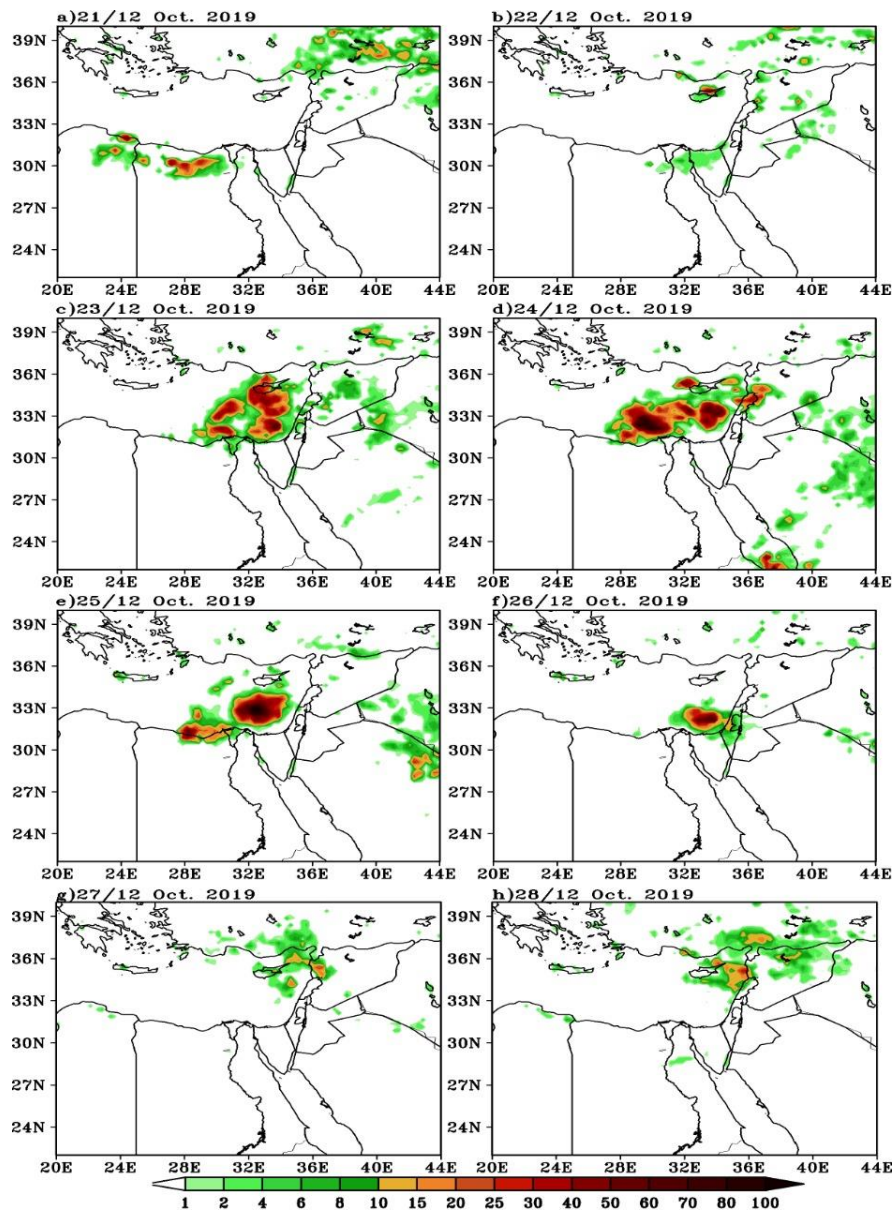


**Figure 4.** The daily spatial rainfall pattern from the TRMM dataset for the period 21–28 October 2019.

GE= gross energy kcal/kg; CP= Crude protein; Ca=Calcium; P=Phosphorus

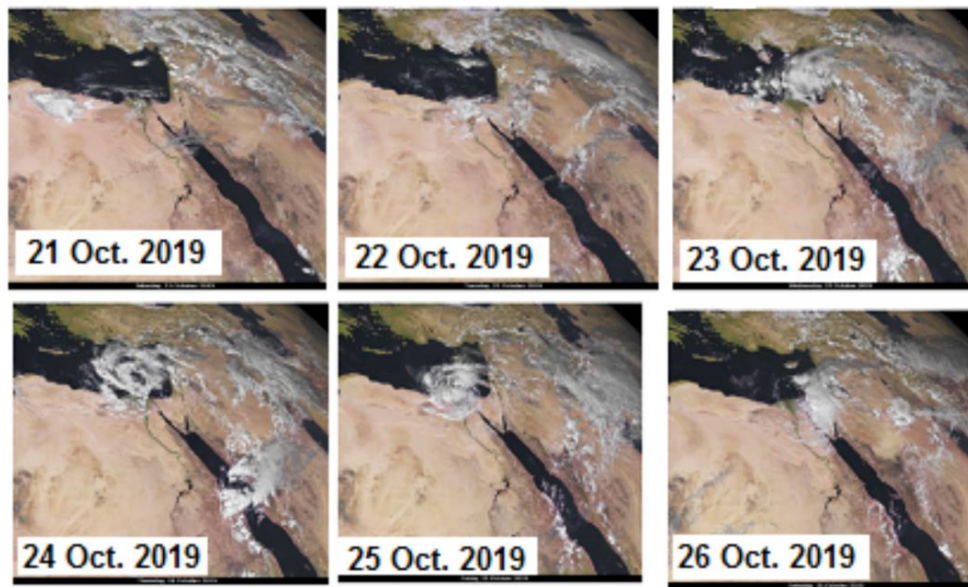


Figure 5: Satellite images of the daily position of Mediane Scott over Eastern Mediterranean for the period 21- 26 October 2019 [Source: Visible (VIS) satellite images getting from EUMETSAT].

2019. The center cuddles the seashore west of Port Said, Egypt. However, rainfall reached the south of Cairo. Table 1 shows the daily composite mean of precipitation rate over Egypt through the period of Mediane Scott. However, a new climatic change record of rainfall over the north coast of Egypt existed through the period of Mediane Scott. Whereas, the anomaly of precipitation rate reaches 11 mm/day above its normal value through October. The normal value of the precipitation rate taken for the period 1981-2010

TABLE 1: THE DAILY PRECIPITATION RATE OVER EGYPT, GEOPOTENTIAL HEIGHT (Z) AND Z ANOMALY AT 500 hPa OVER THE EM AND THE DAILY POSITION OF AITCZ DURING THE PERIOD OF MEDIANE SCOTT (21-27 OCTOBER 2019).

Date Oct. 2019	Precip. (mm)	Location over Egypt	Z(m) at 500 hPa over EM	Anomaly Z(m) at 500 hPa over EM	Location of ITCZ above
21	8	north coast of Sinai	5800	0	13.6° N
22	12	north coast of Sinai	5750	-100	14.0° N
23	25	north coast of Egypt	5700	-150	18.5° N
24	21	north coast of Egypt	5650	-100	21.0° N
25	24	north coast of Egypt	5750	-100	21.0° N
26	14	north coast of Egypt	5800	-100	15.0° N
27	1	north coast of Egypt and Sinai	5750	0	11.5° N

#### 4.2 GEOPOTENTIAL HEIGHT VARIATION AT 500 hPa

The daily NCEP/NCAR reanalysis data of geopotential height over 500 hPa level for the northern hemisphere has been used to analyze the period 21–28 October 2019. Analysis of composite mean and anomaly of the geopotential height data have been performed to illustrate the development and

generation of Mediane Scott over the Eastern Mediterranean through this period. The results of the analysis revealed that there is an extreme distribution of geopotential height at 500 hPa over Europe. The Rossby wave has a meridional extension on 21 October 2019 rather than its normal structure (Figure 1a). On 22 October 2019, an omega-shaped block of this Rossby wave initiated over Europe. The western flank of this block is a

low-pressure system over Morocco. Meanwhile, its eastern flank is a low-pressure system over the Eastern Mediterranean “Medicane Scott”, as can be seen in Figure 1b and Table 1. The Medicane Scott persisted over the Eastern Mediterranean for six days from 22- 26 October and landfall over Egypt from 24- 26 October. The Medicane Scott covered all the northern part of Egypt on 25 October, as demonstrated in Figure 4e and Figure 5. The omega-shaped block persisted over Europe for five days from 22nd to 26th October 2019 as illustrated in Figures 2 and Table 1. Whereas the criteria of the existing blocking episode are the persistence of at least (-100 m) anomaly of geopotential height at the level of 500 hPa level. On 28 October 2019, the omega-shaped block and Medicane Scott dissipated completely from its region of formation in Europe and the Eastern Mediterranean, respectively as illustrated in Figure 2h. Table 1 has the mean daily values of geopotential height and its anomaly values over the Eastern Mediterranean through the period of Medicane Scott. The period of the blocking and the period of Medicane Scott existed from the records.

#### 4.3 AITCZ OSCILLATION DURING THE PERIOD OF STUDY

The AITCZ (15° W – 35° E) mean position data for the last decadal of October 2019 (21-31 October 2019) are used. For Africa, the mean position for every 10 days was calculated for the region from 15° W – 35° E. The ITCZ data series started in 1979 for Africa, and its long-term means are used for the period 1979-2001. Also, visible (VIS) satellite images obtained from EUMETSAT are used to identify the daily African ITCZ position by using cloud clusters through the period 21- 27 October 2019. We found that the decadal latitudinal position of the African ITCZ during the period 21- 31 October 2019 varies from western Africa rather than eastern Africa through this period, as shown in Figure 6. The anomaly of the decadal latitudinal position of the African ITCZ during the period 21- 31 October 2019 is a positive anomaly for all longitudes from 10°W to 35°E. The maximum anomaly of the African ITCZ latitude position reached at 20°E, as shown in Figure 6. The daily position of African ITCZ through the period 21st-27th October 2019 is determined using visible channel satellite images. Figure 6 shows day by day location of ITCZ over Africa through this period. It is clear that the ITCZ varied from day to day and reached its maximum northward shift (21°N) over eastern Africa from 24th and 25th October 2019, as can be seen from Figure 6 and Table 1.

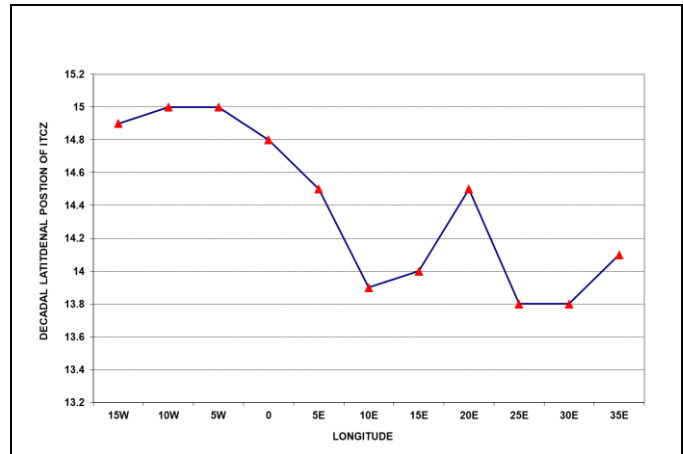


Figure 6: The decadal latitudinal position of the African ITCZ throughout the period 21- 31 October 2019

#### 4.4 RELATIONSHIP BETWEEN RAINFALL AND AITCZ OSCILLATION

Through this section, a correlation coefficient technique is used to apprehend the relationship between precipitation rate over Egypt, geopotential height, and geopotential height anomaly at level 500 hPa over the Eastern Mediterranean and the position of AITCZ during the period of Medicane Scott. It is found that there is an outstanding significant negative correlation (-0.86) between the precipitation over Egypt and the anomaly of geopotential height at 500 hPa level over Eastern Mediterranean through the period of Medicane Scott, as shown in Table 2. There is a highly significant positive correlation (0.93) between the daily precipitation over Egypt and the daily location of the Intertropical Convergence Zone through the period of Medicane Scott, as shown in Table 2. There is a negative correlation (-0.638) between the geopotential height at 500 hPa level over the Eastern Mediterranean and the daily location of the Intertropical Convergence Zone through the period of Medicane Scott, as shown in Table 2. There is a negative correlation (-0.527) between the precipitation over Egypt and the geopotential height at 500 hPa level over the Eastern Mediterranean through the period of Medicane Scott, as illustrated in Table 2.

**Table 2:** Correlation Coefficient matrix of the parameters of daily precip. over Egypt, Z(m) and Z(m) anomaly at 500 hPa over EM and the daily position of during the period of Medicane Scott (21-27 October 2019).

Correlation coefficient	Z (m) at 500 hPa over EM	Z (m) at 500 hPa over EM	Anomaly of Z(m) at 500 hPa over EM	Location of ITCZ
Precip. over Egypt	1	-0.527	-0.861*	0.925**
Z (m) at 500 hPa over EM	-0.527	1	0.471	-0.638
Anomaly of Z(m) at 500 hPa over EM	-0.861*	0.471	1	-0.674
Location of ITCZ	0.925**	-0.638	-0.674	1

\* Significance level is 95%.  
\*\* Significance level is 99%.



#### 4.5 MOISTURE FLUX VARIATION

The interaction between the midlatitude and tropical systems supported the transport of tropical moisture towards the Arabian Peninsula (AP). During 21- 28 October 2019, enhanced moisture is observed over Arabian and Red Seas, equatorial and north-eastern Africa and AP, leading to above-normal relative humidity over the larger part of northern Saudi Arabia on 23- 26 October (Figure 7). In this section we will illustrate the behavior of the divergent and rotational components of the total water vapour flux along with precipitable water content for two tropospheric layers during the period from 23- 26 October. The lower tropospheric layer is taken from 1000 to 850 hPa, while the middle layer from 700 to 500 hPa (Chakraborty et al., 2006; Abdeldym et al., 2019; Al-Mutairi et al., 2019). Figures 8a,d,g,j, Figures 8b,e,h,k illustrate the rotational components of integrated moisture-flux vector along with precipitable water in the two tropospheric layers at 23 to 26 October 2019. While Figures 8c,f,i,L illustrate the divergent components of integrated moisture-flux vector along with precipitable water in the second tropospheric layers for the same period. The divergent component indicates regions of moisture source or sink, while the rotational component describes the atmospheric water vapor transport. In the second tropospheric layer, it is clear that there are three moisture-source regions observed from the divergent component (Figures 8c,f,i,L); the first one is located over the Arabian Sea (including south Red sea, north of Ethiopia and middle of Sudan); the second region locates southeast of Sudan. These source regions supply moisture to the area of interaction (east of Mediterranean and Egypt). The presence of a strong anticyclonic circulation associated with the Azores high over north Africa helping on transporting the moisture to the region of interaction (Figure 2 and Figures 8b,e,h,k). The rotational moisture transport component brings moisture from two regions; the first region appears over the Indian Ocean, Arabian Sea, south of Red Sea and northeast of Sudan. The second source region is the Atlantic and Mediterranean Sea. In the middle layer (Figures 8c,f,i,L), the divergent moisture flux area at 23 October is observed over east Mediterranean countries (Syria, Iraq, east of turkey), while

at 24 and 25 October the areas of divergent moisture flux appear over east and middle east of Europe (its center at 50° N, 35° E). In this layer, the rotational moisture transport component brings a huge amount of moisture with an amount of precipitable water more than 40 mm from two regions; the first source region appears over the Indian Ocean, Arabian Sea, south of Red Sea and north east of Sudan, while the second source region is the Atlantic and Mediterranean Sea (Figures 8b,e,h,k). In the middle layer (Figures 8c,f,i,L), the divergent moisture flux at 23 October is observed over Iran, while at 23 and 24 October the areas of divergent moisture flux appear over south of AP, above and north of turkey and over Libya. Various elongated convergence zones are seen over the area of interaction, the first one (23 October) appears over north of Red sea and east of Sudan while in 24 October the convergence zone extended from north of Iraq to the middle of Red Sea and south west of Sudan. On 25 and 26 October, the convergence zone extended from north and the middle of Red Sea and south east of Sudan. In the upper layer (not shown), the rotational moisture transport component brings a very little amount of moisture from two regions; the first source region is from the north Atlantic through south Europe, while the second source associated with the subtropical jet. The lower and middle tropospheric moisture divergence and the upper tropospheric moisture divergence over east of Mediterranean are indication of the vertical motion of moist air, which in turn may release latent heat due to condensation. This available heat energy may be the source of low-level baroclinic instability. As the cyclone shifts slowly eastward, a divergent moisture flux area is observed over east Mediterranean region at lower tropospheric layer (23 October), while over the same region in the middle tropospheric layer there is a convergent moisture flux which indicates downward motion. However, the strong divergence area of available moisture over north and middle of EM in the lower tropospheric layer corresponding to strong convergence over the same area in the upper layer may explain the heavy rainfall during 24 and 25 October (Figure 4). The upper-tropospheric convergence over EM and Iraq associated with the upper level moisture transport may have a considerable influence on precipitation over this region at during 24 and 25 October

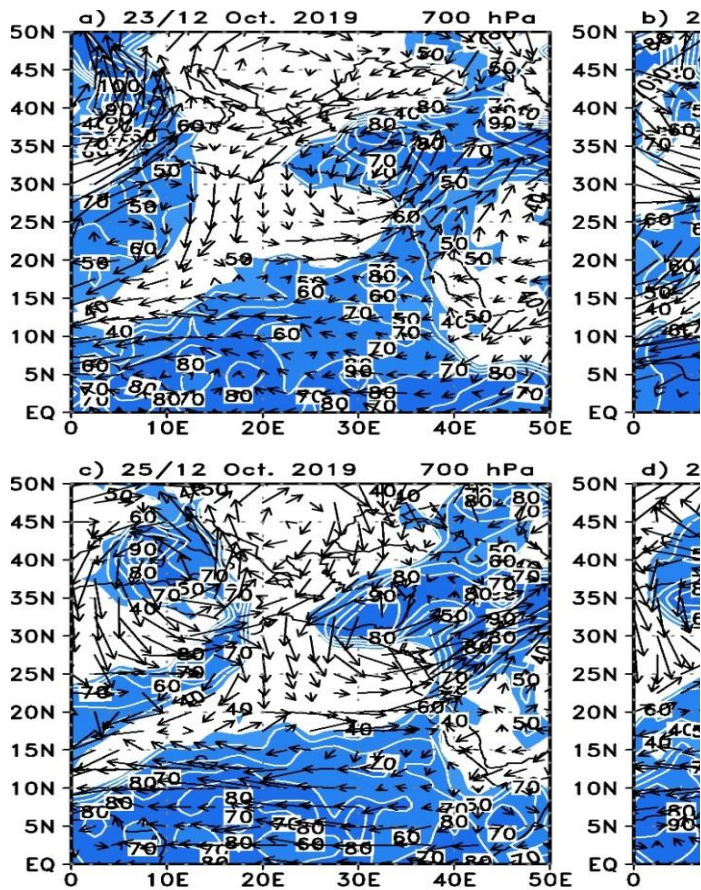


Figure 7. Relative humidity (shaded; %) at 700 hPa, that greater than 30 % contour interval is 10 % and wind in vectors.

## 5. CONCLUSION

Egypt suffered from extreme storms like tropical storms. In late October 2019, Medcane Scott developed over the Eastern Mediterranean region and landfall over Egypt. This Medcane invaded Egypt with extreme amounts of rainfall not recorded over Egypt before. The daily precipitation over the north coast of Egypt reached 20 mm/day on October 25<sup>th</sup>, 2019. This record of precipitation is a new climatic record for October over Egypt. However, no historical records of Mediterranean Medcane exist over the Eastern Mediterranean region and landfall occurs over Egypt rather than Medcane Scott. Through the present research, the relationship between the development of Medcane Scott and AITCZ has been challenged. The results revealed there is a direct positive strong significant

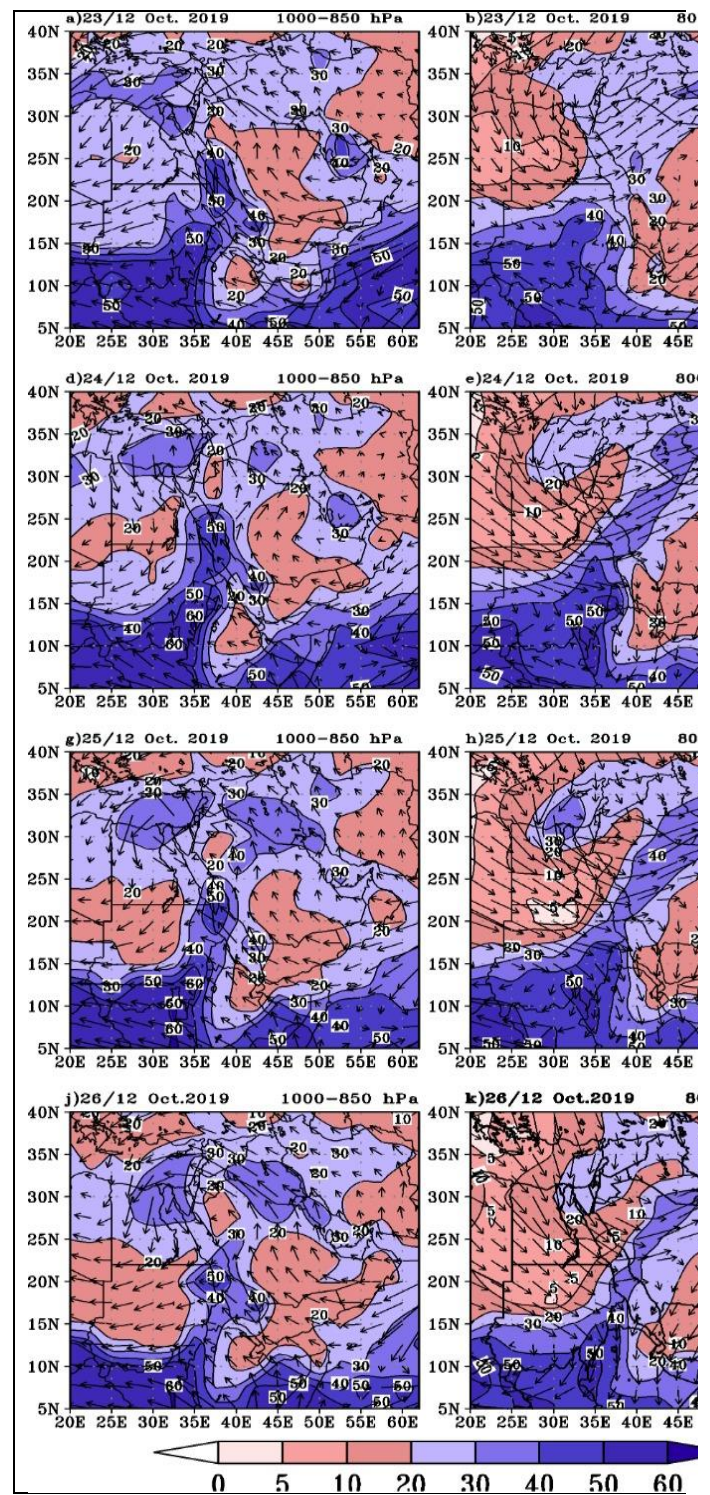


Figure 8. Rotational component of integrated moisture-flux (vector;  $\text{kg m}^{-1} \text{s}^{-1}$ ) along with precipitable water content (shaded; mm) in the two tropospheric layers: the lower layer with 1000–850 hPa (a,d,g,j) and the middle layer with 800–500 hPa (b,e,h,k) for 12Z on 23–26 October 2019. Also, Divergent component of integrated moisture-flux vector for the middle layer with 800–500 hPa (c,f,i,l) for 12Z of 23–26 October 2019. The colored regions are the divergent (source) and convergent (sink) component of the moisture flux ( $10^{-3} \text{ kg m}^{-2} \text{ s}^{-1}$ ).

correlation of 0.93 between the precipitation over Egypt and the AITCZ through the period 21<sup>st</sup>-27<sup>th</sup> October 2019.

Moreover, there is an extremely northward shift of AITCZ mainly over the north Sudan and central part of the Red Sea through the period of Mediane Scott. This northward shift of AITCZ over the eastern part of Africa controls and persists the Rossby wave over Europe. The persistence of the Rossby wave over Europe leads to the development of an omega-shaped block over that region. Whereas, the Mediane Scott in the Eastern Mediterranean is the eastern flank of this block. One can conclude that interaction between AITCZ and the midlatitudes Rossby wave existed causing the development of Mediane Scott that landfall over Egypt on October 2019. Finally, a strong teleconnection between the tropical weather regime AITCZ and the midlatitude weather regime of the Rossby wave is obtained. This teleconnection creates an omega-shaped blocking system that persists over Europe and leads to the development of Mediane Scott that landfall in Egypt in October 2019

#### DATA AVAILABILITY

NCEP/NCAR reanalysis datasets of daily precipitation rates are available at <https://psl.noaa.gov/data/composites/datasets.html>. A monthly/seasonal meantime series of the precipitation rate from the NCEP reanalysis dataset is available at <https://psl.noaa.gov/cgi-bin/data/timeseries/timeseries1.pl>. The datasets of AITCZ are available at the Climate Prediction Centre from its website [http://www.cpc.ncep.noaa.gov/products/monitoring\\_data/](http://www.cpc.ncep.noaa.gov/products/monitoring_data/).

#### ACKNOWLEDGMENTS

It is a pleasure for the authors in expressing deep gratitude to the Climate Diagnostics Centre for providing the data to support the present study. Plots and images are provided from the NOAA-CIRES Climate Diagnostics Centre, Boulder, Colorado, the USA from the website of <http://www.cdc.noaa.gov>. Also, I would like to thank the Climate Prediction Centre for supporting the latitudinal position data of African ITCZ which is obtained from the website [http://www.cpc.ncep.noaa.gov/products/monitoring\\_data](http://www.cpc.ncep.noaa.gov/products/monitoring_data). Finally, thanks to EUMETSAT for support of satellite images

#### REFERENCES

- [1] Barriopedro D, Fischer EM, Luterbacher J, et al (2011) The hot summer of 2010: redrawing the temperature record map of Europe. *Science* (80- ) 332:220–224
- [2] BLASKOVIC T. (2019) MEDICANE "SCOTT" MAKES LANDFALL OVER EGYPT, HEAVY RAIN SPREADING THROUGH THE REGION. WATCHERS. NEWS. ON OCTOBER 26, 2019.
- [3] Bonett DG, Wright TA (2000) Sample size requirements for estimating Pearson, Kendall and Spearman correlations. *Psychometrika* 65:23–28
- [4] Cavicchia L, von Storch H, Gualdi S (2014) A long-term climatology of medicanes. *Clim Dyn* 43:1183–1195
- [5] Chan SC, Evans JL (2002) Comparison of the structure of the ITCZ in the west Pacific during the boreal summers of 1989–93 using AMIP simulations and ECMWF reanalysis. *J Clim* 15:3549–3568
- [6] Diao Y, Li J, Luo D (2006) A new blocking index and its application: Blocking action in the Northern Hemisphere. *J Clim* 19:4819–4839
- [7] Dole RM, Gordon ND (1983) Persistent anomalies of the extratropical Northern Hemisphere wintertime circulation: Geographical distribution and regional persistence characteristics. *Mon Weather Rev* 111:1567–1586
- [8] Emanuel K (2005) Genesis and maintenance of "Mediterranean hurricanes". *Adv Geosci* 2:217–220
- [9] Fita L, Flaounas E (2018) Medicanes as subtropical cyclones: the December 2005 case from the perspective of surface pressure tendency diagnostics and atmospheric water budget. *Q J R Meteorol Soc* 144:1028–1044
- [10] Gaertner MÁ, González-Alemán JJ, Romera R, et al (2018) Simulation of medicanes over the Mediterranean Sea in a regional climate model ensemble: impact of ocean–atmosphere coupling and increased resolution. *Clim Dyn* 51:1041–1057
- [11] Hafez Y (2012a) Variability of intertropical convergence zone (ITCZ) and extreme weather events. *Atmos Model Appl* 111
- [12] Hafez Y (2012b) Blocking systems persist over north hemisphere and its role in extreme hot waves over Russia during summer 2010. *Atmos Model Appl* 137
- [13] Hafez Y, Labban A (2018) The Role Played by Blocking System over North America on the Development of Hurricane Ophelia over North Atlantic Ocean. *J Geosci Environ Prot* 6:1
- [14] Hafez Y (2016) Study on the relationship between the oceanic nino index and surface air temperature and precipitation rate over the Kingdom of Saudi Arabia. *J Geosci Environ Prot* 4:146
- [15] Hafez YY (2008) The role played by blocking over the Northern Hemisphere on Hurricane Katrina. *J Am Sci* 4:10–25
- [16] Hafez YY, Almazroui M (2016) Study of the relationship between African ITCZ variability and an extreme heat wave on Egypt in summer 2015. *Arab J Geosci* 9:476
- [17] Hafez YY, Hasanean HM, Hussein MA (2020) A blocking diagnosis method and its application in the blocking system over Europe in the Summer of 2010. *Asia-Pacific J Atmos Sci* 1–16
- [18] Ilesanmi OO (1971) An empirical formulation of an ITD rainfall model for the tropics: a case study of Nigeria. *J Appl Meteorol* 10:882–891
- [19] Jafari M, Lashkari H (2020) Study of the relationship between the intertropical convergence zone expansion and the precipitation in the southern half of Iran. *J Atmos Solar-Terrestrial Phys* 210:105439
- [20] Mazza E, Ulbrich U, Klein R (2017) The tropical transition of the October 1996 mediane in the western Mediterranean Sea: A warm seclusion event. *Mon Weather Rev* 145:2575–2595
- [21] [3] Miglietta MM, Mastrangelo D, Conte D (2015) Influence of physics parameterization schemes on the simulation of a tropical-like cyclone in the Mediterranean Sea. *Atmos Res* 153:360–375
- [22] [3] Moscatello A, Miglietta MM, Rotunno R (2008) Numerical analysis of a Mediterranean hurricane over southeastern Italy. *Mon Weather Rev* 136:4373–4397
- [23] Mudzwiti M (2019) Egypt braces for more wind, rain from ‘mediane’. *Techfinancials*
- [24] NewsRhodes University. Johannesburg Metropolitan Area Johannesburg Metropolitan Area · Associate editor @ Techfinancials SA · Techfinancials News.
- [25] Rex DF (1951) The effect of Atlantic blocking action upon European climate. *Tellus* 3:100–112
- [26] Ricchi A, Miglietta MM, Bonaldo D, et al (2019) Multi-physics

- ensemble versus Atmosphere--Ocean coupled model simulations for a tropical-like cyclone in the Mediterranean Sea. *Atmosphere (Basel)* 10:202
- [27] Romera R, Gaertner MÁ, Sánchez E, et al (2017) Climate change projections of medicanes with a large multi-model ensemble of regional climate models. *Glob Planet Change* 151:134–143
- [28] Tonks, Sara; Miller, Brandon (2019) "A rare hurricane-like storm in the Mediterranean threatens Egypt and Israel". Edition.cnn.com. CNN. Retrieved 1 November 2019.
- [29] Waliser DE, Gautier C (1993) A satellite-derived climatology of the ITCZ. *J Clim* 6:2162–2174
- [30] Woollings T, Barriopedro D, Methven J, et al (2018) Blocking and its response to climate change. *Curr Clim Chang Reports* 4:287–300
- [31] Hersbach, H., Bell, B., Berrisford, P., Hirahara, S., Horányi, A., Muñoz-Sabater, J., Nicolas, J., Peubey, C., Radu, R., Schepers, D. and Simmons, A., 2020. The ERA5 global reanalysis. *Quarterly Journal of the Royal Meteorological Society*, 146(730), pp.1999-2049.
- [32] Huffman, G.J., Adler, R.F., Bolvin, D.T. and Nelkin, E.J., 2010. The TRMM multi-satellite precipitation analysis (TMPA). In *Satellite rainfall applications for surface hydrology* (pp. 3-22). Springer, Dordrecht.
- [33] Chakraborty, A., Behera, S.K., Mujumdar, M., Ohba, R. and Yamagata, T., 2006. Diagnosis of tropospheric moisture over Saudi Arabia and influences of IOD and ENSO. *Monthly Weather Review*, 134(2), pp.598-617.
- [34] Rosen, R.D., Salstein, D.A., Peixoto, J.P., 1979. Variability in the annual fields of large-scale atmospheric water vapor transport. *Mon. Wea. Rev.* 107, 26–37.
- [35] Chen, T.C., 1985. Global water vapor flux and maintenance during FGGE. *Mon. Wea. Rev.* 113, 1801–1819.
- [36] Abdeldym, A., Basset, H.A., Sayad, T. and Morsy, M., 2019. Kinetic energy budget and moisture flux convergence analysis during interaction between two cyclonic systems: Case study. *Dynamics of Atmospheres and Oceans*, 86, pp.73-89.
- [37] Al-Mutairi, M., Abdel Basset, H., Morsy, M. and Abdeldym, A., 2019. On the Effect of Red Sea and Topography on Rainfall over Saudi Arabia: Case Study. *Atmosphere*, 10(11), p.669.
- [38] KRISHNAMURTI, T. N., BOUNOUA, L., & ANDREJCZUK, M. (1997). AN INTRODUCTION TO NUMERICAL WEATHER PREDICTION TECHNIQUES. *PURE AND APPLIED GEOPHYSICS*, 149(4), 830-831 LAYING HENS. *REVISTA BRASILEIRA DE ZOOTECNIA* 45: 518-523. [HTTPS://DOI.ORG/10.1590/S1806-92902016000900003](https://doi.org/10.1590/S1806-92902016000900003)

## العلاقة بين منطقة التقارب الإفريقية المدارية وتطور عاصفة "سكوت" الطبية على شرق البحر الأبيض المتوسط: دراسة حالة

عبدالحليم بن حسين لبنان  
جامعة الملك عبدالعزيز - كلية الأرصاد والبيئة  
وزراعة المناطق الجافة - قسم الأرصاد - جدة

مستخلص. تبحث الدراسة الحالية في الدور الذي تلعبه منطقة التحول بين المداري الأفريقية (AITCZ) في تطوير عاصفة ميديكان سكوت المطرية فوق مصر خلال الفترة من ٢١ إلى ٢٧ أكتوبر ٢٠١٩. تم استخدام البيانات العقدية واليومية من AITCZ لشهر أكتوبر ٢٠١٩. تم استخدام طرق تحليل السلاسل الزمنية والشذوذ ومعامل الارتباط لتحليل مجموعات البيانات هذه. تكشف النتائج أن هناك امتداداً ملحوظاً شمالاً لـ AITCZ ، بشكل رئيسي على شرق إفريقيا خلال فترة عاصفة ميديكان سكوت. هناك علاقة ارتباط موجبة قوية (٠,٩٢٥) بين هطول الأمطار اليومي فوق مصر والموقع العرضي للجزء الشرقي من AITCZ خلال فترة عاصفة ميديكان سكوت. يتحكم AITCZ في استمرار موجة روسبي فوق أوروبا ومناطق شرق البحر الأبيض المتوسط مما تسبب في كتلة على شكل أوميغا فوق الجزء الجنوبي من أوروبا. ومع ذلك، فإن الجناح الشرقي من هذه الكتلة ميديكان سكوت الذي يهب فوق مصر والذي يرتبط بطقس ممطر شديد غير طبيعي فوق مصر.

**كلمات مفتاحية:** عاصفة ميديكان سكوت، معدل هطول الأمطار، أوميغا بلوك، مصر، البحر الأبيض المتوسط

## العلاقة بين منطقة التقارب الإفريقية المدارية وتطور عاصفة "سكوت" الطبية على شرق البحر الأبيض المتوسط: دراسة حالة

عبدالحليم بن حسين لبنان

جامعة الملك عبدالعزيز - كلية الأرصاء والبيئة وزراعة المناطق الجافة - قسم الأرصاء - جدة

تبحث الدراسة الحالية في الدور الذي تلعبه منطقة التحول بين المداري الإفريقية (AITCZ) في تطوير عاصفة ميديكان سكوت المطرية فوق مصر خلال الفترة من ٢١ إلى ٢٧ أكتوبر ٢٠١٩. تم استخدام البيانات العقدية واليومية من AITCZ لشهر أكتوبر ٢٠١٩. تم استخدام طرق تحليل السلاسل الزمنية والشذوذ ومعامل الارتباط لتحليل مجموعات البيانات هذه. تكشف النتائج أن هناك امتداداً ملحوظاً شمالاً لـ AITCZ ، بشكل رئيسي على شرق إفريقيا خلال فترة عاصفة ميديكان سكوت. هناك علاقة ارتباط موجبة قوية (٠,٩٢٥) بين هطول الأمطار اليومي فوق مصر والموقع العرضي للجزء الشرقي من AITCZ خلال فترة عاصفة ميديكان سكوت. يتحكم AITCZ في استمرار موجة روسبي فوق أوروبا ومناطق شرق البحر الأبيض المتوسط مما تسبب في كتلة على شكل أوميغا فوق الجزء الجنوبي من أوروبا. ومع ذلك، فإن الجناح الشرقي من هذه الكتلة ميديكان سكوت الذي يهب فوق مصر والذي يرتبط بطقس ممطر شديد غير طبيعي فوق مصر.

**كلمات مفتاحية:** عاصفة ميديكان سكوت، معدل هطول الأمطار، أوميغا بلوك، مصر، البحر الأبيض المتوسط